Acta Crystallographica Section C
Crystal Structure Communications
ISSN 0108-2701

Seven 3-methylidene-1*H*-indol-2(3*H*)-ones related to the multiple-receptor tyrosine kinase inhibitor sunitinib

John Spencer,[a] Babur Z. Chowdhry,[a] Samiyah Hamid,[a] Andrew P. Mendham,[a] Louise Male,[b]*‡ Simon J. Coles[b] and Michael B. Hursthouse[b]

[a]School of Science, University of Greenwich at Medway, Central Avenue, Chatham, Kent ME4 4TB, England, and [b]EPSRC National Crystallography Service, School of Chemistry, University of Southampton, Highfield, Southampton SO17 1BJ, England
Correspondence e-mail: l.male@bham.ac.uk

Received 9 July 2009
Accepted 15 December 2009
Online 15 January 2010

The solid-state structures of a series of seven substituted 3-methylidene-1*H*-indol-2(3*H*)-one derivatives have been determined by single-crystal X-ray diffraction and are compared in detail. Six of the structures {(3*Z*)-3-(1*H*-pyrrol-2-ylmethylidene)-1*H*-indol-2(3*H*)-one, $C_{13}H_{10}N_2O$, (2*a*); (3*Z*)-3-(2-thienylmethylidene)-1*H*-indol-2(3*H*)-one, $C_{13}H_9NOS$, (2*b*); (3*E*)-3-(2-furylmethylidene)-1*H*-indol-2(3*H*)-one monohydrate, $C_{13}H_9NO_2\cdot H_2O$, (3*a*); 3-(1-methylethylidene)-1*H*-indol-2(3*H*)-one, $C_{11}H_{11}NO$, (4*a*); 3-cyclohexylidene-1*H*-indol-2(3*H*)-one, $C_{14}H_{15}NO$, (4*c*); and spiro[1,3-dioxane-2,3′-indolin]-2′-one, $C_{11}H_{11}NO_3$, (5)} display, as expected, intermolecular hydrogen bonding (N—H···O=C) between the 1*H*-indol-2(3*H*)-one units. However, methyl 3-(1-methylethylidene)-2-oxo-2,3-dihydro-1*H*-indole-1-carboxylate, $C_{13}H_{13}NO_3$, (4*b*), a carbamate analogue of (4*a*) lacking an N—H bond, displays no intermolecular hydrogen bonding. The structure of (4*a*) contains three molecules in the asymmetric unit, while (4*b*) and (4*c*) both contain two independent molecules.

Comment

Conformational restriction is a useful tactic employed in medicinal chemistry, which often leads to an improvement in the biological properties of a molecule by reducing entropy and contributing to enhanced binding to a receptor or enzyme. This extends to the presence of a conformational blocker, such as an *ortho*-substituent in biphenyl derivatives, which hinders free rotation, or a strong hydrogen bond to 'lock' two groups together into a favourable binding orientation. A strategically placed double bond (*E* or *Z* isomer) in the molecule also falls within this category, since it can drastically affect the activity or affinity of ligands binding to enzymes or receptors (Patrick, 2009; King, 2002). Sunitinib, (1), is a conformationally restricted clinically approved MRTKI (multi-receptor tyrosine kinase inhibitor) anticancer drug, combining a 1*H*-indol-2(3*H*)-one (oxindole) core with a *Z*-substituted 3-(1*H*-pyrrol-2-ylmethylidene) side chain (Fig. 1; Atkins *et al.*, 2006). The pyrrole NH group in (1) forms an intramolecular hydrogen bond with the oxindole carbonyl group, evidenced in solution, by ^{1}H NMR spectroscopy, and in the cocrystal structure of (1) bound to an RTK (receptor tyrosine kinase) (Mohammadi *et al.*, 1997). Compound (2*a*), a lead molecule in the design of (1), exhibits biological activity towards kinases [IC_{50} = 0.39 m*M*, PDGF (platelet-derived growth factor)], whereas the 1-methylpyrrole analogue (*E*)-(3*b*) exhibits drastically reduced biological activity (IC_{50} > 100 m*M*) towards PDGF (Sun *et al.*, 1998; Boiadjiev & Lightner, 2003).

Given the strong correlation between stereochemistry and kinase inhibitory action within this series of molecules, we have undertaken a structural study of oxindole analogues in the solid phase to complement the extensive prior studies undertaken in solution (Sun *et al.*, 1998). Our investigation of compounds (2)–(4) by Raman and FT–IR spectroscopy (Spencer *et al.*, 2010), supported by theoretical calculations (Kausar *et al.*, 2009; Bell *et al.*, 2007), has been facilitated by structure determinations from single-crystal X-ray diffraction analysis, reported here. The molecules selected for this study can be subdivided into several categories:

(i) heterocycle-substituted analogues (2), found to exist exclusively as the *Z* isomer in solution;

(ii) heterocycle-substituted analogues (3), found to exist exclusively as the *E* isomer in solution;

(iii) simple symmetrically substituted analogues (4) and (5), obtained in order to provide a fingerprint region for the FT–IR and Raman studies, especially (4*a*), given that the parent methylidene compound (4*d*) is reported to be unstable in solution (Rossiter, 2002).

Analogues (2)–(4) were synthesized by a standard Knoevenagel condensation of oxindole with a variety of aldehydes

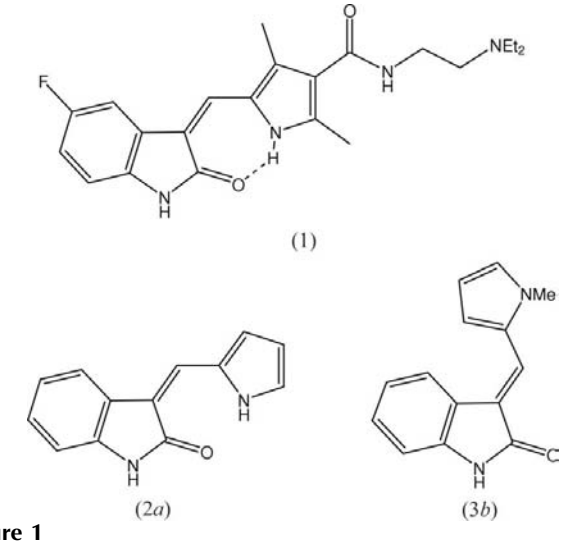

Figure 1
Examples of oxindoles tested for anticancer activity.

‡ Current address: School of Chemistry, University of Birmingham, Edgbaston, Birmingham B15 2TT, England.

or ketones under both thermal (oil bath; Sun *et al.*, 1998, 2003; Maskell *et al.*, 2007) and microwave conditions (Villemin & Martin, 1998; Zhang & Go, 2009) (see *Experimental* and supplementary information for details of synthetic optimization studies and extraction and purification procedures). Compound (4*b*) was synthesized from (4*a*) by reaction with dimethyl carbonate (Trost *et al.*, 2007). Compound (5) was purchased from Maybridge Chemicals. Crystals of (2*a*), (2*b*), (3*a*), (4*a*)–(4*c*) and (5), of suitable quality for analysis by single-crystal X-ray diffraction, were grown from dichloromethane/hexane. The molecular structures are shown in Figs. 2–8, while selected bond lengths and angles are given in Table 1. The structure of (5) determined at room temperature has been published previously (De & Kitagawa, 1991). The geometry of the structure reported here, determined at 120 K, corresponds very closely with that of the previously reported structure.

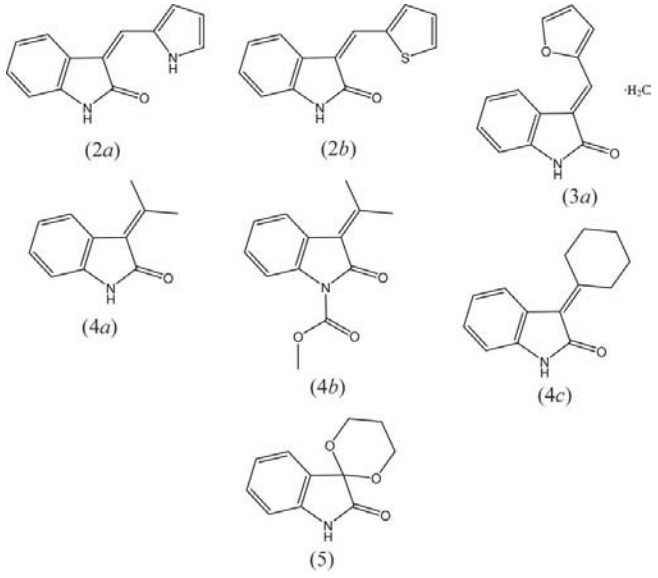

In the following discussion, atom X*y* refers also to X100+*y* and X200+*y* in structures where Z' is greater than 1 [(4*a*)–(4*c*)].

The geometry of the oxindole portion of the molecules is generally very similar for all seven structures, and compares

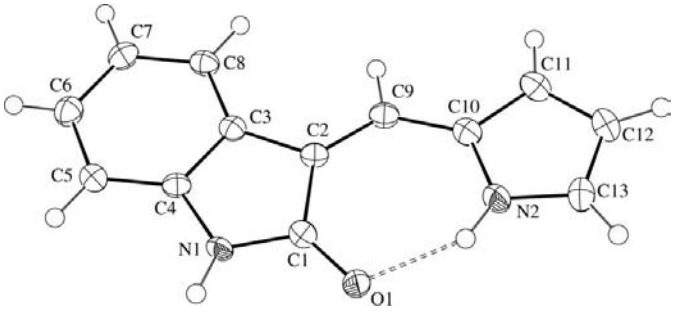

Figure 2
The molecular structure of (2*a*), showing the atom-numbering scheme. Displacement ellipsoids are drawn at the 50% probability level and H atoms are shown as small spheres of arbitrary radii. The dashed line indicates the intramolecular hydrogen bond.

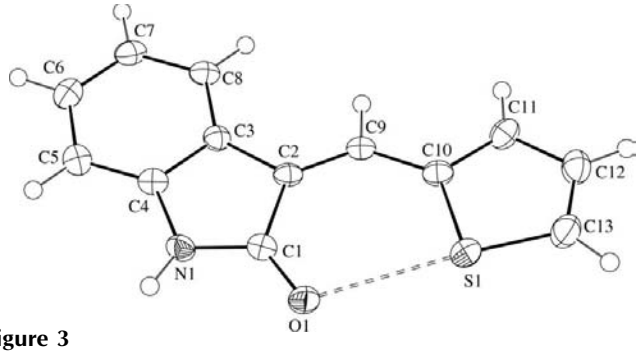

Figure 3
The molecular structure of (2*b*), showing the atom-numbering scheme. Displacement ellipsoids are drawn at the 50% probability level and H atoms are shown as small spheres of arbitrary radii. The dashed line indicates the intramolecular hydrogen bond.

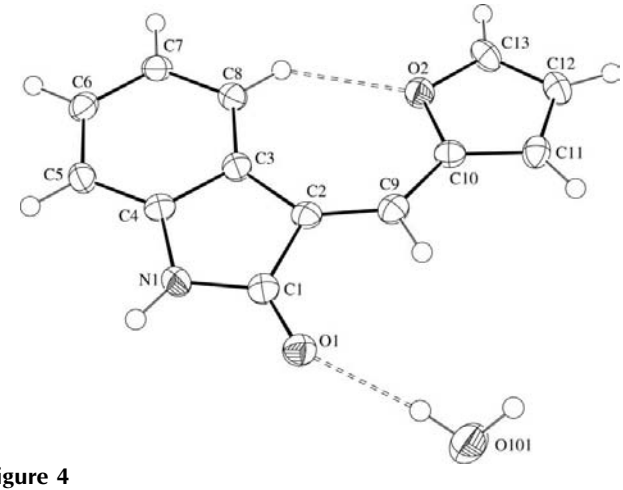

Figure 4
The molecular structure of (3*a*), showing the atom-numbering scheme. Displacement ellipsoids are drawn at the 50% probability level and H atoms are shown as small spheres of arbitrary radii. Dashed lines indicate hydrogen bonds.

closely with oxindole fragments found in a search of the Cambridge Structural Database (CSD, Version 5.30 with November 2008 and February 2009 updates; Allen, 2002). However, the only structure in which atom N1 is substituted, (4*b*), displays significantly longer N1—C1 and N1—C4 distances, a shorter O1—C1 distance and a smaller C1—N1—C4 angle compared with the other six structures (Table 1). Also, the only structure in which atom C2 is sp^3 hybridized, (5), displays significantly longer C1—C2 and C2—C3 bond lengths compared with the other six structures.

By comparing the six structures in which atom C2 is sp^2 hybridized, we have observed differences in the heterocycle-substituted analogues (2*a*), (2*b*) and (3*a*), where atom C10 is sp^2 hybridized, compared with structures (4*a*), (4*b*) and (4*c*), where atom C10 is sp^3 hybridized. It is interesting to note that, while structures (2*a*), (2*b*) and (3*a*) are all in the orthorhombic crystal system and have just one molecule in the asymmetric unit (Z' = 1), the remaining structures all occupy lower-symmetry crystal systems and have $Z' > 1$ [Z' = 3 for (4*a*), and Z' = 2 for (4*b*) and (4*c*)]. The heterocycle-substituted oxindoles determined by Boiadjiev & Lightner (2003), namely (3*Z*)-[(4,5-dimethylpyrrol-2-yl)methylidenyl]indolin-2-one and (3*E*)-

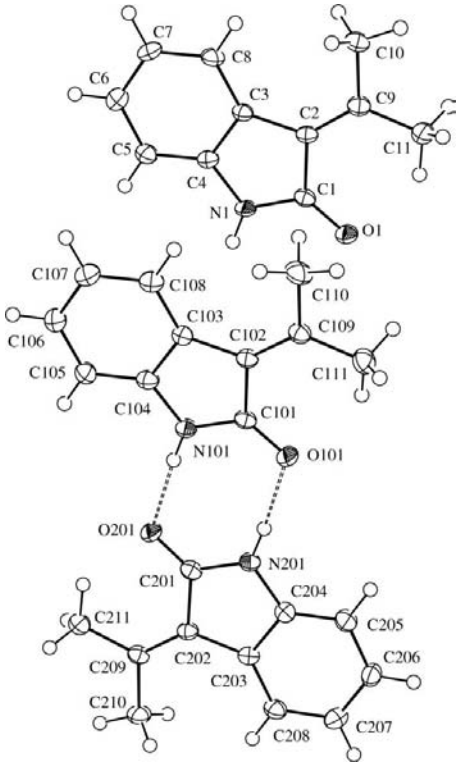

Figure 5
The independent molecules of (4*a*), showing the atom-numbering scheme. Displacement ellipsoids are drawn at the 50% probability level and H atoms are shown as small spheres of arbitrary radii. Dashed lines indicate hydrogen bonds.

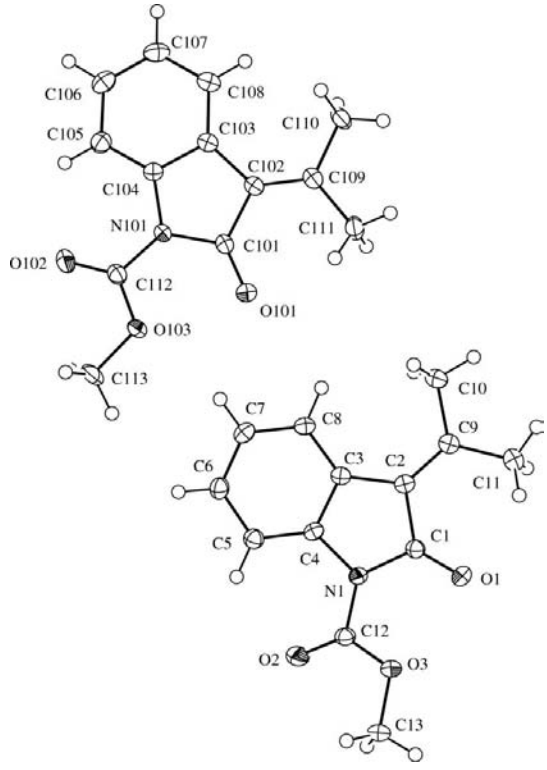

Figure 6
The independent molecules of (4*b*), showing the atom-numbering scheme. Displacement ellipsoids are drawn at the 50% probability level and H atoms are shown as small spheres of arbitrary radii.

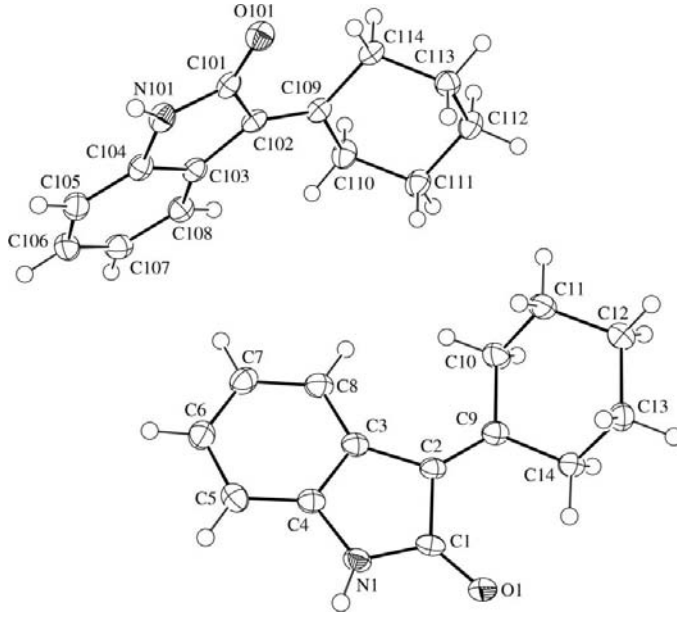

Figure 7
The independent molecules of (4*c*), showing the atom-numbering scheme. Displacement ellipsoids are drawn at the 50% probability level and H atoms are shown as small spheres of arbitrary radii.

[(1-methylpyrrol-2-yl)methylidenyl]indolin-2-one, also have $Z' = 1$. However, a search of the CSD revealed that this trend is not observed in all substituted oxindoles and we must thus conclude that the fact that (4*a*)–(4*c*) have $Z' > 1$ is based on a number of different factors.

In addition to the more obvious geometric differences between the heterocycle-substituted analogues and structures (4*a*), (4*b*) and (4*c*), it is found that the average C1—C2 bond distance in (4*a*) and (4*c*) [1.509 (2) Å] is significantly longer than that in (2*a*), (2*b*) and (3*a*) [1.488 (2) Å], while in (4*b*) (in which atom N1 is substituted) it is only slightly longer at 1.490 (8) Å. In the heterocycle-substituted oxindoles determined by Boiadjiev & Lightner (2003), the average of the equivalent of the C1—C2 bond distance is 1.474 (3) Å, shorter than in any of the seven structures reported here. In turn, the average of the equivalent distance to N1—C1 reported by Boiadjiev & Lightner is somewhat longer [1.372 (3) Å] than the average for (2*a*), (2*b*), (3*a*), (4*a*), (4*c*) and (5) [1.359 (5) Å]. It is postulated that these differences arise from the differing temperatures at which the single-crystal X-ray data sets were collected, 298 K for the Boiadjiev & Lightner structures and 120 K for those reported here.

The solid-state structures agree with the results from solution NMR studies (see supplementary information) in that structures (2*a*) and (2*b*) exist as *Z* isomers [average C1—C2—C9 bond angle = 128.6 (2)°], while (3*a*) exists as the *E* isomer [C1—C2—C9 = 118.9 (2)°]. These angles compare well with the equivalent angles in the *Z* and *E* isomers reported by Boiadjiev & Lightner (2003), 128.3 (3) and 117.5 (5)°, respectively. The formation of the *Z* isomers in (2*a*) and (2*b*) can be attributed to intramolecular N—H···O [in 2*a*)] and

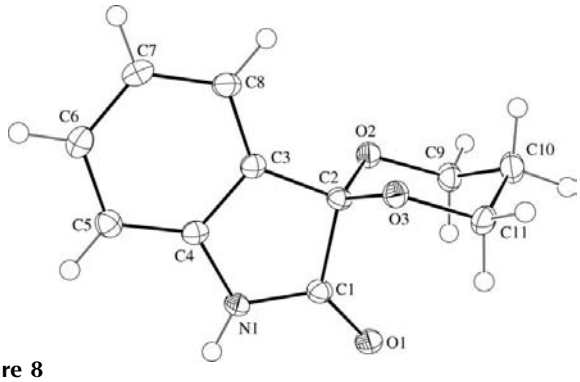

Figure 8
The molecular structure of (5), showing the atom-numbering scheme. Displacement ellipsoids are drawn at the 50% probability level and H atoms are shown as small spheres of arbitrary radii.

O···S (Réthoré *et al.*, 2007) [in (2*b*)] interactions, while in (3*a*) the lack of a suitable group to form an intramolecular interaction with atom O1, combined with the formation of a weak C—H···O contact (C8—H8···O2), makes the adoption of the *E* isomer more favourable (Table 3).

The oxindole portion of all seven structures is highly planar, while the entire molecule does not generally deviate far from planarity for (2*a*), (2*b*), (3*a*), (4*a*) and (4*b*), and this seems to be related to the formation of intramolecular interactions between groups in the oxindole and substituent portions of the molecules (Tables 1 and 3, and Table S3 in the supplementary information). By contrast, the *E* isomer reported by Boiadjiev & Lightner (2003) has no suitable groups with which to form intramolecular interactions and the molecule is much more twisted than in the structures reported here, with the angle between the planes through the oxindole and substituent portions being approximately 30° (*cf.* Table S3). In (4*c*), the formation of weak intramolecular C—H···O interactions involving atoms C14 and C114 (Table 3) corresponds with an average C1—C2—C9—C10 torsion angle which is relatively close to 180° (Table 1). It seems that the formation of even weak C—H···O interactions has a significant effect on the conformation of these molecules in the solid state.

Structures (2*a*), (2*b*), (3*a*), (4*a*), (4*c*) and (5) are also affected by the formation of intermolecular hydrogen bonds involving the oxindole N—H and C═O units, which leads to the formation of molecular dimers in every case (Fig. 9–11, Figs. S1–S4 in the supplementary information, and Table 2). The hydrogen-bonding motif leading to the formation of the molecular dimers can be described as an $R_2^2(8)$ ring (Etter *et al.*, 1990). Analysis of Fig. 11 shows that, while the dimers formed in (3*a*), (4*a*) and (4*c*) are fairly planar [not taking into account the conformation of the cyclohexyl rings in (4*c*)], the molecules forming the dimers in (2*a*), (2*b*) and (5) are quite staggered with respect to one another. This is borne out by analysis of the N—H···O hydrogen-bond angles (Table 2). While the average for the interactions in (2*a*), (2*b*) and (5) is 163 (3)°, the average for those in (3*a*), (4*a*) and (4*c*) is significantly larger at 172 (3)°.

Structure (3*a*) is the only one of the seven to incorporate a molecule of solvent in the crystal structure. This water molecule is involved in hydrogen bonding both to the oxindole C═O group and to other water molecules (Fig. 9 and Table 2). The molecular dimers in this structure are connected with one another *via* π–π stacking interactions (Hunter & Sanders, 1990), the parallel dimer planes being separated by 3.3 Å, while atom O1 and the N1/C1–C4 ring form a lone-pair–π interaction (Mooibroek *et al.*, 2008) (O1···ring centroid =

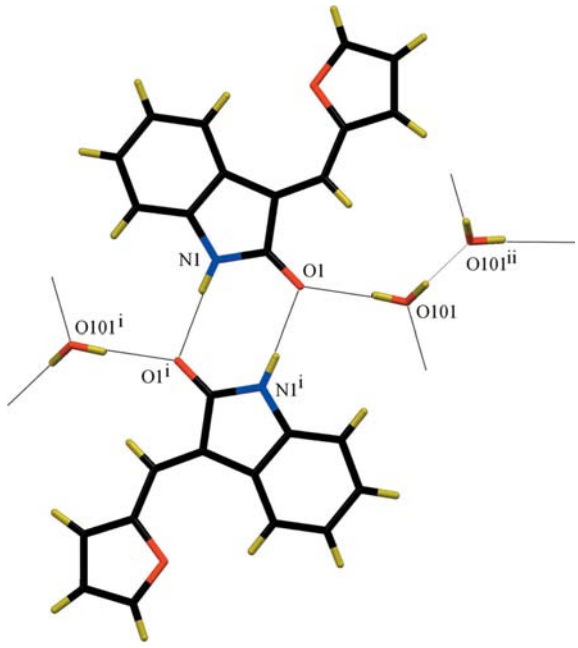

Figure 9
A view of the hydrogen-bonded dimer and hydrogen bonding (thin lines) involving the solvent water molecule in the structure of (3*a*). [Symmetry codes: (i) $1-x, -1-y, -z$; (ii) $\frac{1}{2}-x, \frac{1}{2}+y, z$.]

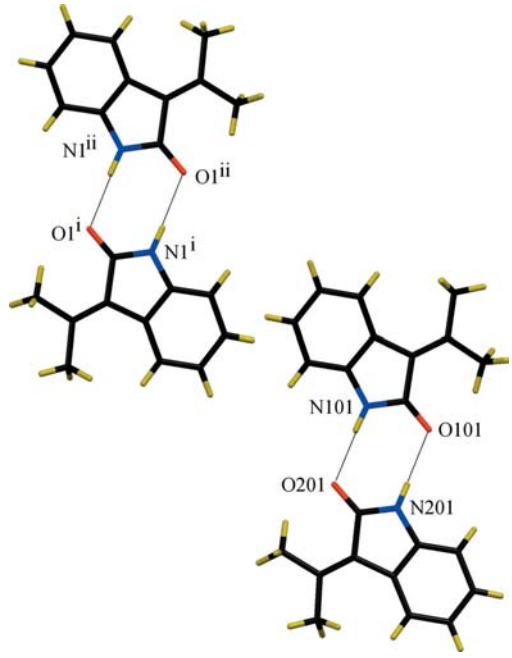

Figure 10
A view of the two hydrogen-bonded dimers (thin lines) formed in the structure of (4*a*). [Symmetry codes: (i) $1-x, -y, 1-z$; (ii) $-1+x, y, z$.]

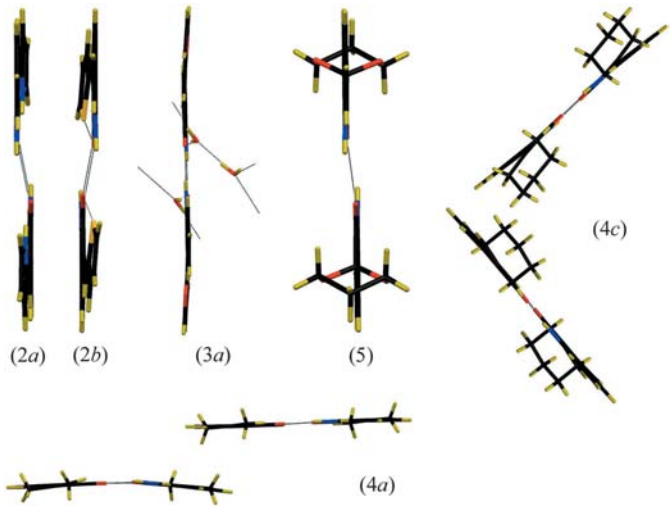

Figure 11
Side views of the hydrogen-bonded dimers (thin lines) formed in the structures of (2*a*), (2*b*), (3*a*), (4*a*), (4*c*) and (5).

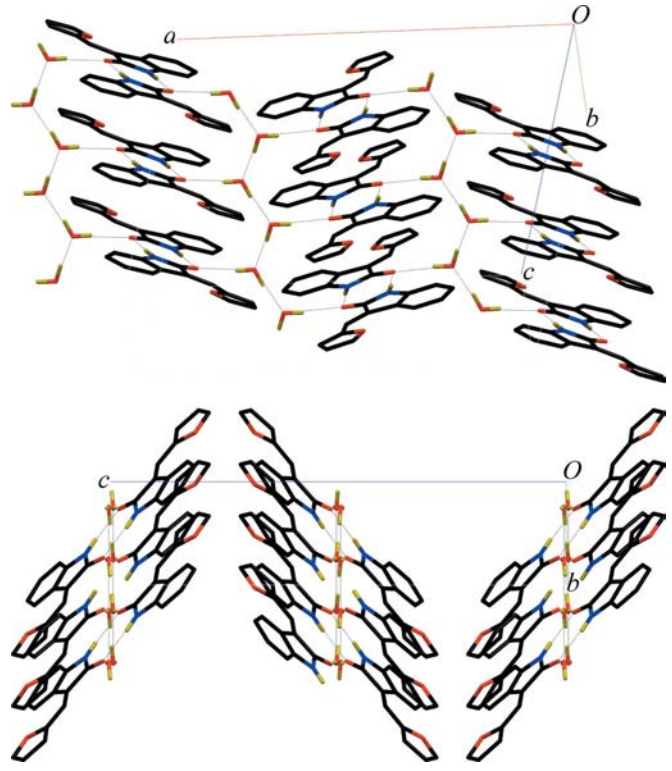

Figure 12
The packing of the hydrogen-bonded dimers (thin lines) in (3*a*). Only those H atoms involved in hydrogen bonding are shown.

3.2 Å and C1—O1···ring centroid = 92°). This stacking of dimers leads to the formation of columns along the (010) direction which are connected to one another in the (100) direction *via* hydrogen bonding with the water molecules (Fig. 12).

The delocalized bonding and planar nature of these molecules mean that the other six structures also exhibit varying degrees of π–π stacking interactions, with interplanar distances ranging from 3.1 Å in (4*c*) to approximately 3.6 Å in (2*b*) (Figs. S5–S10 in the supplementary information).

In conclusion, the X-ray single-crystal structure determinations described here have brought to light a number of interesting properties in oxindoles in the solid phase, including high Z' values and inter- and intramolecular hydrogen bonding. This offers the potential for synthesizing oxindoles with extended molecular architectures and biological properties (Spencer *et al.*, 2009) and will be of continuing invaluable assistance to theoretical calculations (Kausar *et al.*, 2009).

Experimental

The starting materials for the syntheses of the title compounds were purchased from commercial sources (Sigma–Aldrich, Fisher, Fluorochem and Frontier Scientific) and were used without further purification. All reactions were carried out in air, and commercial grade solvents and materials were used except where specified. Elemental analyses were performed on a CE Instruments Eager 300 apparatus. Crystals of each of compounds (2*a*)–(5) of sufficient quality for X-ray diffraction analysis were obtained by the diffusion of hexane into a CH_2Cl_2 solution.

Synthetic and purification procedure for (2a). 1,3-Dihydro-2*H*-indol-2-one (oxindole) (0.319 g, 2.40 mmol) and 1*H*-pyrrole-2-carbaldehyde (0.190 g, 2.00 mmol) were added to EtOH (5 ml) with 2–3 drops of piperidine as a catalyst. The reaction mixture was refluxed until complete according to thin-layer chromatographic (TLC) monitoring, which equates to approximately 3 h. The reaction mixture was cooled to room temperature and, on further cooling with ice, afforded a precipitate. The crude product was obtained by filtration and washed with cold EtOH. Product (2*a*) was purified by column chromatography on silica with chloroform–methanol (90:10 *v*/*v*) as eluant. Crystals of (2*a*) were obtained as a yellow solid (yield 0.420 g, 84%; m.p. 483–486 K). Analysis found: C 73.0, H 4.9, N 13.6%; $C_{13}H_{10}N_2O{\cdot}0.05CH_2Cl_2$ requires: C 73.1, H 4.7, N 13.1%. While the empirical formula was found to contain a very small amount of CH_2Cl_2 by elemental analysis and NMR, no dichloromethane was found in the crystal structure.

Synthetic and purification procedure for (2b). Oxindole (0.133 g, 1.00 mmol) and thiophene-2-carbaldehyde (0.159 g, 1.20 mmol) were reacted, and purification was achieved as for (2*a*), except that hexane–ethyl acetate (50:50 *v*/*v*) was used as eluant during chromatographic purification. Crystals of (2*b*) were obtained as a yellow solid (yield 0.178 g, 79%; m.p. 463–466 K). Analysis found: C 68.9, H 4.2, N 6.2%; $C_{13}H_9NOS$ requires: C 68.7, H 4.0, N 6.2%.

Synthetic and purification procedure for (3a). Oxindole (0.133 g, 1.00 mmol) and 2-furaldehyde (0.115 g, 1.20 mmol) were reacted, and purification was achieved as for (2*a*), except that hexane–ethyl acetate (50:50 *v*/*v*) was used as eluant for chromatographic purification. Crystals of (3*a*) were obtained as a yellow solid [yield 0.166 g, 79%; m.p. 443–446 K (literature value 451 K; Villemin & Martin, 1998)]. Analysis found: C 67.9, H 4.7, N 6.8%; $C_{13}H_{11}NO_3{\cdot}H_2O$ requires: C 68.1, H 4.8, N 6.1%.

Synthetic and purification procedure for (4a). Oxindole (0.133 g, 1.00 mmol) and acetone (7.90 g, 136 mmol) were reacted, and purification was achieved as for (2*a*), except that chloroform–ethyl acetate (50:50 *v*/*v*) was used as eluant. Crystals of (4*a*) were obtained as an orange solid (yield 0.158 g, 92%; m.p. 459–461 K). Analysis found: C 76.2, H 6.5, N 8.3%; $C_{11}H_{11}NO$ requires: C 76.3, H 6.4, N 8.1%.

Synthetic and purification procedure for (4b). Compound (4*b*) was made according to a published method (Trost *et al.*, 2007) [m.p. 341–342 K (literature value 341–343 K)]. Analysis found: C 76.4, H 5.7, N 5.9%; $C_{13}H_{13}NO_3$ requires: C 76.2, H 5.7, N 6.0%.

Synthetic and purification procedure for (4c). Oxindole (0.319 g, 2.40 mmol) and cyclohexanone (0.196 g, 2.00 mmol) were reacted, and purification was achieved as for (2*a*), except that chloroform–ethyl acetate (50:50 *v*/*v*) was used as eluant. Crystals of (4*c*) were obtained as a brown solid [yield 0.450 g, 88%; m.p. 458–460 K [literature value 464 K (Villemin & Martin, 1998)]. Analysis found: C 75.8, H 6.9, N 6.3%; $C_{14}H_{15}NO{\cdot}0.1CH_2Cl_2$ requires: C 76.3, H 6.9, N 6.3%. While the empirical formula was found to contain a very small amount of CH_2Cl_2 by elemental analysis and NMR, no dichloromethane was found in the crystal structure.

Synthetic and purification procedure for (5). Compound (5) was purchased from Maybridge Chemicals.

Microwave-mediated syntheses of analogues (2)–(4) (Spencer, 2007, 2008). Oxindole (1 mmol), the aldehyde or ketone (1.5 equivalents), ethanol (5 ml) and piperidine (2 drops) were placed in a sealable microwave tube and heated to 423 K for 30 min using continuous cooling (P_{max}) in a CEM Discover unit. After cooling the reaction mixture, the crude product was subjected to the same work-up as for the thermal-mediated route.

Compound (2*a*)

Crystal data

$C_{13}H_{10}N_2O$
M_r = 210.23
Orthorhombic, *Pbca*
a = 14.6031 (6) Å
b = 6.2725 (3) Å
c = 22.6997 (12) Å
V = 2079.25 (17) Å^3
Z = 8
Mo *K*α radiation
μ = 0.09 mm^{-1}
T = 120 K
0.28 × 0.10 × 0.01 mm

Data collection

Bruker–Nonius Roper CCD camera on κ-goniostat diffractometer
Absorption correction: multi-scan (*SADABS*; Sheldrick, 2007)
T_{min} = 0.976, T_{max} = 0.999
15759 measured reflections
1828 independent reflections
1412 reflections with $I > 2\sigma(I)$
R_{int} = 0.085

Refinement

$R[F^2 > 2\sigma(F^2)]$ = 0.053
$wR(F^2)$ = 0.110
S = 1.05
1828 reflections
145 parameters
H-atom parameters constrained
Δρ$_{max}$ = 0.18 e Å^{-3}
Δρ$_{min}$ = −0.22 e Å^{-3}

Compound (2*b*)

Crystal data

$C_{13}H_9NOS$
M_r = 227.27
Orthorhombic, *Pbcn*
a = 11.9297 (5) Å
b = 10.8294 (6) Å
c = 16.6986 (9) Å
V = 2157.32 (19) Å^3
Z = 8
Mo *K*α radiation
μ = 0.27 mm^{-1}
T = 120 K
0.16 × 0.08 × 0.04 mm

Data collection

Bruker–Nonius APEXII CCD camera on κ-goniostat diffractometer
Absorption correction: multi-scan (*SADABS*; Sheldrick, 2007)
T_{min} = 0.958, T_{max} = 0.989
18202 measured reflections
2463 independent reflections
2024 reflections with $I > 2\sigma(I)$
R_{int} = 0.052

Refinement

$R[F^2 > 2\sigma(F^2)]$ = 0.054
$wR(F^2)$ = 0.125
S = 1.09
2463 reflections
145 parameters
H-atom parameters constrained
Δρ$_{max}$ = 0.34 e Å^{-3}
Δρ$_{min}$ = −0.42 e Å^{-3}

Compound (3*a*)

Crystal data

$C_{13}H_9NO_2{\cdot}H_2O$
M_r = 229.23
Orthorhombic, *Pbcn*
a = 19.2250 (7) Å
b = 5.0503 (3) Å
c = 22.1886 (14) Å
V = 2154.3 (2) Å^3
Z = 8
Mo *K*α radiation
μ = 0.10 mm^{-1}
T = 120 K
0.30 × 0.06 × 0.04 mm

Data collection

Bruker–Nonius Roper CCD camera on κ-goniostat diffractometer
Absorption correction: multi-scan (*SADABS*; Sheldrick, 2007)
T_{min} = 0.970, T_{max} = 0.996
13065 measured reflections
1881 independent reflections
1355 reflections with $I > 2\sigma(I)$
R_{int} = 0.085

Refinement

$R[F^2 > 2\sigma(F^2)]$ = 0.052
$wR(F^2)$ = 0.118
S = 1.06
1881 reflections
160 parameters
3 restraints
H atoms treated by a mixture of independent and constrained refinement
Δρ$_{max}$ = 0.24 e Å^{-3}
Δρ$_{min}$ = −0.25 e Å^{-3}

Compound (4*a*)

Crystal data

$C_{11}H_{11}NO$
M_r = 173.21
Triclinic, $P\overline{1}$
a = 9.7504 (3) Å
b = 10.2281 (3) Å
c = 14.0530 (5) Å
α = 95.766 (2)°
β = 107.842 (2)°
γ = 96.617 (2)°
V = 1311.45 (7) Å^3
Z = 6
Mo *K*α radiation
μ = 0.09 mm^{-1}
T = 120 K
0.30 × 0.08 × 0.04 mm

Data collection

Bruker–Nonius APEXII CCD camera on κ-goniostat diffractometer
Absorption correction: multi-scan (*SADABS*; Sheldrick, 2007)
T_{min} = 0.975, T_{max} = 0.997
21390 measured reflections
5972 independent reflections
4122 reflections with $I > 2\sigma(I)$
R_{int} = 0.059

Refinement

$R[F^2 > 2\sigma(F^2)]$ = 0.079
$wR(F^2)$ = 0.168
S = 1.08
5972 reflections
358 parameters
H-atom parameters constrained
Δρ$_{max}$ = 0.36 e Å^{-3}
Δρ$_{min}$ = −0.31 e Å^{-3}

Compound (4*b*)

Crystal data

$C_{13}H_{13}NO_3$
M_r = 231.24
Monoclinic, $P2_1/n$
a = 10.6939 (2) Å
b = 17.2595 (4) Å
c = 12.7714 (3) Å
β = 108.3220 (10)°
V = 2237.73 (8) Å^3
Z = 8
Mo *K*α radiation
μ = 0.10 mm^{-1}
T = 120 K
0.36 × 0.30 × 0.18 mm

Table 1
Selected bond lengths (Å), angles (°) and torsion angles (°) from structures (2*a*), (2*b*), (3*a*), (4*a*)–(4*c*) and (5).

	(2*a*)	(2*b*)	(3*a*)	(4*a*)†	(4*b*)†	(4*c*)†	(5)
N1—C1	1.358 (3)	1.366 (3)	1.352 (3)	1.360 (3)	1.4335 (7)	1.3605 (7)	1.3519 (16)
N1—C4	1.396 (3)	1.405 (3)	1.406 (3)	1.393 (3)	1.426 (3)	1.398 (2)	1.4082 (16)
O1—C1	1.250 (2)	1.240 (3)	1.246 (3)	1.2337 (15)	1.2114 (14)	1.2350 (14)	1.2298 (15)
C1—C2	1.486 (3)	1.488 (3)	1.489 (3)	1.510 (2)	1.490 (8)	1.5075 (7)	1.5670 (16)
C2—C3	1.467 (3)	1.463 (3)	1.477 (3)	1.4730 (10)	1.464 (3)	1.485 (2)	1.5053 (16)
C3—C4	1.401 (3)	1.401 (3)	1.408 (3)	1.406 (2)	1.4070 (14)	1.4075 (7)	1.3935 (17)
C2—C9/C2—O2‡	1.360 (3)	1.352 (3)	1.353 (3)	1.352 (2)	1.3560 (14)	1.3535 (7)	1.4093 (15)
C9—C10/C2—O3‡	1.424 (3)	1.432 (3)	1.414 (3)	1.503 (4)	1.5045 (7)	1.510 (6)	1.4096 (14)
C1—N1—C4	111.60 (17)	111.20 (19)	111.0 (2)	111.90 (17)	109.7 (3)	111.8 (3)	111.91 (10)
C1—C2—C9/C1—C2—O2‡	128.77 (19)	128.5 (2)	118.9 (2)	124.9 (4)	123.1 (3)	124.3 (4)	111.85 (9)
C2—C9—C10/C2—O2—C9‡	131.5 (2)	134.1 (2)	133.2 (2)	122.03 (15)	121.325 (7)	123.2 (2)	113.62 (9)
C1—C2—C9—C10/C1—C2—O2—C9‡	−2.6 (4)	−2.6 (4)	176.8 (2)	−177 (3)	179.57 (7)	170.4 (19)	−72.13 (12)
C2—C9—C10—*X*/C2—O2—C9—C10§	0.3 (4)	−3.3 (4)	−0.4 (4)				−54.98 (13)

† The reported values are averages of the parameters from the different crystallographically independent molecules in the asymmetric unit. ‡ For structure (5), the second parameter is reported, while for the remaining six structures the first parameter is given. § In (2*a*), *X* = N2, in (2*b*) *X* = S1 and in (3*a*) *X* = O2, and the second parameter is reported for structure (5).

Table 2
Intermolecular hydrogen-bonding interactions (Å, °) in (2*a*), (2*b*), (3*a*), (4*a*), (4*c*) and (5).

Structure	Interaction	*D*—H	H···*A*	*D*···*A*	*D*—H···*A*
(2*a*)	N1—H1···O1^{i}	0.88	1.99	2.841 (2)	162
(2*b*)	N1—H1···O1^{ii}	0.88	1.99	2.835 (2)	160
(3*a*)	N1—H1···O1^{iii}	0.88	1.95	2.828 (3)	174
	O101—H1*W*···O101^{iv}	0.87 (2)	1.90 (2)	2.763 (2)	172 (3)
	O101—H2*W*···O1	0.86 (2)	2.00 (2)	2.852 (2)	173 (3)
(4*a*)	N1—H1···O1^{v}	0.88	1.98	2.859 (3)	174
	N101—H101···O201	0.88	1.96	2.837 (3)	176
	N201—H201···O101	0.88	1.98	2.848 (3)	170
(4*c*)	N1—H1···O1^{vi}	0.88	1.97	2.846 (2)	171
	N101—H101···O101^{v}	0.88	1.98	2.850 (2)	169
(5)	N1—H1···O1^{v}	0.88	1.98	2.844 (1)	165

Symmetry codes: (i) $-x+1, -y, -z+1$; (ii) $-x+1, -y+1, -z+1$; (iii) $-x+1, -y-1, -z$; (iv) $-x+\frac{1}{2}, y+\frac{1}{2}, z$; (v) $-x+2, -y, -z+1$; (vi) $-x+3, -y+1, -z$.

Data collection

Bruker–Nonius Roper CCD camera on κ-goniostat diffractometer
Absorption correction: multi-scan (*SADABS*; Sheldrick, 2007)
T_{min} = 0.966, T_{max} = 0.983
26778 measured reflections
5129 independent reflections
3809 reflections with $I > 2\sigma(I)$
R_{int} = 0.052

Refinement

$R[F^2 > 2\sigma(F^2)]$ = 0.049
$wR(F^2)$ = 0.134
S = 1.04
5129 reflections
313 parameters
H-atom parameters constrained
$\Delta\rho_{max}$ = 0.31 e Å^{-3}
$\Delta\rho_{min}$ = −0.35 e Å^{-3}

Compound (4*c*)

Crystal data

$C_{14}H_{15}NO$
M_r = 213.27
Triclinic, $P\overline{1}$
a = 5.3732 (1) Å
b = 13.4962 (4) Å
c = 15.8088 (5) Å
α = 95.3890 (10)°
β = 98.498 (2)°
γ = 101.201 (2)°
V = 1103.32 (5) Å^3
Z = 4
Mo *Kα* radiation
μ = 0.08 mm^{-1}
T = 120 K
0.85 × 0.08 × 0.06 mm

Data collection

Bruker–Nonius APEXII CCD camera on κ-goniostat diffractometer
Absorption correction: multi-scan (*SADABS*; Sheldrick, 2007)
T_{min} = 0.935, T_{max} = 0.995
18503 measured reflections
4997 independent reflections
3778 reflections with $I > 2\sigma(I)$
R_{int} = 0.059

Refinement

$R[F^2 > 2\sigma(F^2)]$ = 0.066
$wR(F^2)$ = 0.135
S = 1.07
4997 reflections
289 parameters
H-atom parameters constrained
$\Delta\rho_{max}$ = 0.33 e Å^{-3}
$\Delta\rho_{min}$ = −0.24 e Å^{-3}

Compound (5)

Crystal data

$C_{11}H_{11}NO_3$
M_r = 205.21
Monoclinic, $P2_1/c$
a = 9.5406 (2) Å
b = 8.4295 (2) Å
c = 12.4103 (3) Å
β = 101.956 (2)°
V = 976.42 (4) Å^3
Z = 4
Mo *Kα* radiation
μ = 0.10 mm^{-1}
T = 120 K
0.50 × 0.40 × 0.36 mm

Table 3
Intramolecular hydrogen-bonding and weak interactions (Å, °) in (2*a*), (2*b*), (3*a*) and (4*a*)–(4*c*).

Structure	Interaction	*D*—H	H···*A*	*D*···*A*	*D*—H···*A*
(2*a*)	N2—H2···O1	0.88	1.89	2.668 (2)	147
(2*b*)	S1···O1			2.792 (2)	
(3*a*)	C8—H8···O2	0.95	2.29	3.035 (3)	135
(4*a*)	C11—H11*A*···O1	0.98	2.18	2.970 (3)	137
	C111—H11*G*···O101	0.98	2.19	2.953 (3)	134
	C211—H21*D*···O201	0.98	2.16	2.961 (3)	137
(4*b*)	C5—H5···O2	0.95	2.27	2.845 (2)	118
	C105—H105···O102	0.95	2.28	2.847 (2)	118
	C11—H11*A*···O1	0.98	2.27	2.879 (2)	119
	C111—H11*D*···O101	0.98	2.32	2.869 (2)	115
(4*c*)	C14—H14*B*···O1	0.99	2.16	2.957 (3)	136
	C114—H11*K*···O101	0.99	2.15	2.953 (3)	137

Data collection

Bruker Nonius Roper CCD camera on κ-goniostat diffractometer	12504 measured reflections 2227 independent reflections
Absorption correction: multi-scan (*SADABS*; Sheldrick, 2007)	1885 reflections with $I > 2\sigma(I)$
$T_{min} = 0.951$, $T_{max} = 0.964$	$R_{int} = 0.032$

Refinement

$R[F^2 > 2\sigma(F^2)] = 0.039$	136 parameters
$wR(F^2) = 0.103$	H-atom parameters constrained
$S = 1.03$	$\Delta\rho_{max} = 0.25$ e Å^{-3}
2227 reflections	$\Delta\rho_{min} = -0.26$ e Å^{-3}

The water H atoms in (3*a*) were located in an electron-density map and their positions refined subject to O—H [0.85 (2) Å] and H···H [1.37 (2) Å] distance restraints, with U_{iso}(H) = 1.5U_{eq}(O). All other H atoms were added at calculated positions and refined using a riding model, with C—H = 0.95 Å for aromatic, 0.99 Å for methylene or 0.98 Å for methyl H atoms and N—H = 0.88 Å, with U_{iso}(H) = 1.5U_{eq}(C) for methyl H atoms and 1.2U_{eq}(C) for aromatic, methylene and N-bound H atoms. In structure (4*a*), the *R* factor is a little high (7.9%). All other indicators of structural quality are good and there is no indication of any twinning or disorder in the structure. It is thought that the explanation may lie in the fact that the variation in the intensities of the diffraction peaks seems to be larger than usual, although the authors cannot be sure that this is the cause.

For all seven compounds, data collection: *COLLECT* (Nonius, 1998); cell refinement: *DENZO* (Otwinowski & Minor, 1997) and *COLLECT*; data reduction: *DENZO* and *COLLECT*; program(s) used to solve structure: *SIR2004* (Burla *et al.*, 2005); program(s) used to refine structure: *SHELXL97* (Sheldrick, 2008); molecular graphics: *ORTEP-3 for Windows* (Version 2.01; Farrugia, 1997) and *Mercury* [Version 1.4.2 (Macrae *et al.*, 2006) and Version 2.2 (Macrae *et al.*, 2008)]; software used to prepare material for publication: *WinGX* (Farrugia, 1999).

The University of Greenwich and GRE are thanked for the provision of CHN analysis facilities and the purchase of an accurate microbalance. Anjum Nazira (University of Greenwich) is thanked for microwave experiments. The EPSRC National Mass Spectrometry Service Centre, University of Wales, Swansea, is thanked for carrying out the HRMS measurements. Colin Stephen is thanked for assistance with graphics and invaluable support.

Supplementary data for this paper are available from the IUCr electronic archives (Reference: GG3207). Services for accessing these data are described at the back of the journal.

References

Allen, F. H. (2002). *Acta Cryst.* B**58**, 380–388.
Atkins, M., Jones, C. A. & Kirkpatrick, P. (2006). *Nat. Rev. Drug. Discov.* **5**, 279–280.
Bell, S., Dines, T. J., Chowdhry, B. Z. & Withnall, R. (2007). *J. Chem. Educ.* **84**, 1364–1370.
Boiadjiev, S. E. & Lightner, D. A. (2003). *Monatsh. Chem.* **134**, 489–499.
Burla, M. C., Caliandro, R., Camalli, M., Carrozzini, B., Cascarano, G. L., De Caro, L., Giacovazzo, C., Polidori, G. & Spagna, R. (2005). *J. Appl. Cryst.* **38**, 381–388.
De, A. & Kitagawa, Y. (1991). *Acta Cryst.* C**47**, 2179–2181.
Etter, M. C., MacDonald, J. C. & Bernstein, J. (1990). *Acta Cryst.* B**46**, 256–262.
Farrugia, L. J. (1997). *J. Appl. Cryst.* **30**, 565.
Farrugia, L. J. (1999). *J. Appl. Cryst.* **32**, 837–838.
Hunter, C. A. & Sanders, J. K. M. (1990). *J. Am. Chem. Soc.* **112**, 5525–5534.
Kausar, N., Alexander, B. D., Dines, T. J., Withnall, R. & Chowdhry, B. Z. (2009). *J. Raman Spectrosc.* **40**, 661–669.
King, F. D. (2002). Editor. *Medicinal Chemistry, Principles and Practice*, 2nd ed. London: RSC.
Macrae, C. F., Bruno, I. J., Chisholm, J. A., Edgington, P. R., McCabe, P., Pidcock, E., Rodriguez-Monge, L., Taylor, R., van de Streek, J. & Wood, P. A. (2008). *J. Appl. Cryst.* **41**, 466–470.
Macrae, C. F., Edgington, P. R., McCabe, P., Pidcock, E., Shields, G. P., Taylor, R., Towler, M. & van de Streek, J. (2006). *J. Appl. Cryst.* **39**, 453–457.
Maskell, L., Blanche, E. A., Colucci, M. A., Whatmore, J. L. & Moody, C. J. (2007). *Bioorg. Med. Chem. Lett.* **17**, 1575–1578.
Mohammadi, M., McMahon, G., Sun, L., Tang, P. C., Hirth, P., Yeh, B. K., Hubbard, S. R. & Schlessinger, J. (1997). *Science*, **276**, 955–960.
Mooibroek, T. J., Gamez, P. & Reedijk, J. (2008). *CrystEngComm*, **10**, 1501–1515.
Nonius (1998). *COLLECT*. Nonius BV, Delft, The Netherlands.
Otwinowski, Z. & Minor, W. (1997). *Methods in Enzymology*, Vol. 276, *Macromolecular Crystallography*, Part A, edited by C. W. Carter Jr & R. M. Sweet, pp. 307–326. New York: Academic Press.
Patrick, G. L. (2009). *An Introduction to Medicinal Chemistry*, 4th ed. Oxford University Press.
Réthoré, C., Madalan, A., Fourmigué, M., Canadell, E., Lopes, E. B., Almeida, M., Clérac, R. & Avarvari, N. (2007). *New J. Chem.* **31**, 1468–1483.
Rossiter, S. (2002). *Tetrahedron Lett.* **43**, 4671–4673.
Sheldrick, G. M. (2007). *SADABS*. University of Göttingen, Germany.
Sheldrick, G. M. (2008). *Acta Cryst.* A**64**, 112–122.
Spencer, J., Dines, T. J., Alexander, B. D., Chowdhry, B. Z., Hamid, S. & Mendham, A. P. (2010). In preparation.
Spencer, J., Mendham, P. M., Kotha, A. K., Richardson, S. C. W., Hillard, E. A., Jaouen, G., Male, L. & Hursthouse, M. B. (2009). *Dalton Trans.* pp. 918–921.
Spencer, J., Nazira, A., Patel, H., Rathnam, R. P. & Verma, J. (2007). *Synlett*, pp. 2557–2558.
Spencer, J., Rathnam, R. P., Patel, H. & Nazira, A. (2008). *Tetrahedron*, **64**, 10195–10200.
Sun, L., Liang, C., Shirazian, S., Zhou, Y., Miller, T., Cui, J., Fukuda, J. Y., Chu, J. Y., Nematalla, A., Wang, X., Chen, H., Sistla, A., Luu, T. C., Tang, F., Wei, J. & Tang, C. (2003). *J. Med. Chem.* **46**, 1116–1119.
Sun, L., Tran, N., Tang, F., App, H., Hirth, P., McMahon, G. & Tang, C. (1998). *J. Med. Chem.* **41**, 2588–2603.
Trost, B. M., Cramer, N. & Silverman, S. M. (2007). *J. Am. Chem. Soc.* **129**, 12396–12397.
Villemin, D. & Martin, B. (1998). *Synth. Commun.* **28**, 3201–3208.
Zhang, W. & Go, M.-L. (2009). *Bioorg. Med. Chem.* **17**, 2077–2090.